



This discussion paper is/has been under review for the journal Atmospheric Chemistry and Physics (ACP). Please refer to the corresponding final paper in ACP if available.

Annual evapotranspiration retrieved solely from satellites' vegetation indices for the Eastern Mediterranean

D. Helman¹, I. M. Lensky¹, and A. Givati²

¹Department of Geography and Environment, Bar Ilan University, Ramat-Gan, Israel

²Israeli Hydrological Service, Water Authority, Jerusalem, Israel

Received: 1 March 2015 – Accepted: 12 May 2015 – Published: 8 June 2015

Correspondence to: D. Helman (davidhelman.biu@gmail.com)

Published by Copernicus Publications on behalf of the European Geosciences Union.

Title Page

Abstract

Introduction

Conclusions

References

Tables

Figures



Back

Close

Full Screen / Esc

Printer-friendly Version

Interactive Discussion



Abstract

We present a simple model to retrieve actual evapotranspiration (ET) solely from satellites (PaVI-E). The model is based on empirical relationships between vegetation indices (NDVI and EVI from MODIS) and total annual ET (ET_{Annual}) from 16 FLUXNET sites representing a wide range of plant functional types and ET_{Annual} . The model was applied separately for (a) annual vegetation systems (i.e., croplands and grasslands) and (b) systems with combined annual and perennial vegetation (i.e., woodlands, forests, savannah and shrublands). It explained most of the variance in ET_{Annual} in those systems (71 % for annuals, and 88 % for combined annuals and perennials systems) while multiple regression and modified Temperature and Greenness models using also land surface temperature did not improve its performance ($p > 0.1$). PaVI-E was used to retrieve ET_{Annual} at 250 m spatial resolution for the Eastern Mediterranean from 2000 to 2014. Models' estimates were highly correlated ($R = 0.92$, $p < 0.01$) with ET_{Annual} calculated from water catchments balances along rainfall gradient in the Eastern Mediterranean. They were also comparable to the coarser resolution ET products of MSG (LSA-SAF MSG ETa, 3.1 km) and MODIS (MOD16, 1 km) at 148 Eastern Mediterranean basins with correlation coefficients (R) of 0.75 and 0.77 and relative bias of 5.2 and -5.2% , respectively ($p < 0.001$ for both). The proposed model is expected to contribute to hydrological study in the Eastern Mediterranean assisting in water resource management, which is one of the most valuable resources of this region.

1 Introduction

Actual evapotranspiration (ET) is a primary component of the global water cycle. Its assessment at global and regional scales is essential for forecasting future atmospheric feedback (Jung et al., 2010; Oki and Kanae, 2006; Zemp et al., 2014). Estimating ET at such scales though, is not straightforward and requires the use of models (Chen et al., 2014; Hu et al., 2015; Jung et al., 2009; Trambauer et al., 2014). Data-driven models

ACPD

15, 15397–15429, 2015

Annual ET retrieved solely from satellites' Vis for the EM

D. Helman et al.

Title Page

Abstract

Introduction

Conclusions

References

Tables

Figures



Back

Close

Full Screen / Esc

Printer-friendly Version

Interactive Discussion



using satellite information benefit from a continuous spatio-temporal direct observation (Ma et al., 2014; Shi and Liang, 2014).

Satellite-based ET models are classified into two: (1) empirical, using the relationship between in situ ET and satellites-derived vegetation indices (VIs) (Glenn et al., 2011; Nagler et al., 2012; Tillman et al., 2012) and (2) physical, using surface temperature from satellites to solve energy balance equations (Anderson et al., 2008; Colaizzi et al., 2012). While some models combine the two approaches (Tsarouchi et al., 2014).

Although physical-based models are much more common their performance is comparable to that of the empirical-based models (Glenn et al., 2010). The accuracy of both approaches is within that of the eddy covariance measurements (70–90 %) used for their calibration or validation (Kalma et al., 2008). Yet, the empirical approach is simpler than the physical-based model and requires less additional information.

The basis for the empirical model is the resource optimisation theory. This theory suggests that plants adjust their foliage density to the environmental capacity to support photosynthetic activity and transpiration (Glenn et al., 2010). Accordingly, changes in vegetation foliage cover (and VIs) will affect ET resulting in high ET–VIs correlations. Then, the empirical equation could be used to retrieve ET in space and time.

This approach is mostly used in vegetation systems with annual cycle of growth and drying where VIs define well the phenological stages (Glenn et al., 2011; Helman and Lensky, 2015; Senay et al., 2011). However, in complex systems comprised of annual (i.e. herbaceous) and perennial (i.e. woody) vegetation the model must be adjusted with additional meteorological data (Helman and Lensky, 2015; Maselli et al., 2014).

The main drawback of the empirical-based approach is that it is limited to a specific site and vegetation type (Glenn et al., 2010; Maselli et al., 2014; Nagler et al., 2012). No common relationship was found between ET and VIs for different sites and climatic conditions.

Here we used MODIS VIs and land surface temperature products and eddy covariance ET from 16 FLUXNET sites with different plant functional types to retrieve ET from satellite data alone. We conducted our analysis on annual vegetation systems

Annual ET retrieved solely from satellites' VIs for the EM

D. Helman et al.

Title Page

Abstract

Introduction

Conclusions

References

Tables

Figures



Back

Close

Full Screen / Esc

Printer-friendly Version

Interactive Discussion



Annual ET retrieved solely from satellites' VIs for the EM

D. Helman et al.

Title Page

Abstract

Introduction

Conclusions

References

Tables

Figures



Back

Close

Full Screen / Esc

Printer-friendly Version

Interactive Discussion



and on complex systems comprising annuals and perennials vegetation. Three empirical models were examined: (1) simple regression, (2) multiple regression and (3) modified Temperature and Greenness models with 16 day and mean annual data. We used a performance-simplicity criterion to choose the model to retrieve ET for the Eastern Mediterranean (EM). Estimates were compared with MODIS and MSG ET operational products and evaluated against ET calculated from water catchments balances in the EM.

2 Data

2.1 Evapotranspiration from eddy covariance towers

In situ ET was derived from eddy covariance towers that constitute the international flux towers net (FLUXNET). Two open FLUXNET sources were used to acquire the datasets: the Oak Ridge National Laboratory Distributed Active Archive Centre (available online (<http://fluxnet.ornl.gov>) from ORNL DAAC, Oak Ridge, Tennessee, USA) and the European fluxes database (<http://gaia.agraria.unitus.it/home>). Half-hourly level 4 ET data were checked for acceptable quality (Reichstein et al., 2005) and gap-filled using methods described in Reichstein et al. (2005) and Moffat et al. (2007). Then, data were aggregated to 16 days means (mm d^{-1}) and total annual ET (mm yr^{-1}). Only ET data since the time MODIS VIs products are available were used (i.e. since 2000).

2.2 Satellite products

We used 16 day NDVI and EVI at a spatial resolution of 250 m (MOD13Q1) and 8 day LST at 1 km spatial resolution (MOD11A2) from MODIS on board Terra satellite. Although Terra provides LST twice a day (around 10.30 a.m./p.m. LT) here we used only daytime LST, which is the relevant for ET processes. The 8 day LST was averaged to match the 16 day temporal resolution of the VIs product.

The MODIS 16 day VIs product is a composite of a single day value selected from 16 days period based on a maximum value criterion (Huete et al., 2002). It represents well the vegetation status of the entire 16 day period because of the gradual development of the vegetation. This enables regressing this MODIS VIs product against 16 day averages of ET. NDVI is defined as (Rouse et al., 1974):

$$\text{NDVI} = \frac{R_{0.8} - R_{0.6}}{R_{0.8} + R_{0.6}}, \quad (1)$$

and EVI as (Huete et al., 2002):

$$\text{EVI} = 2.5 \times \frac{R_{0.8} - R_{0.6}}{R_{0.8} + 6R_{0.6} - 7.5R_{0.5} + 1}, \quad (2)$$

where $R_{0.8}$, $R_{0.6}$ and $R_{0.5}$ are the reflectance at near infrared (0.8 μm), red (0.6 μm) and blue (0.5 μm) bands, respectively. NDVI suffers from asymptotic problems (saturation) over high density of vegetation biomass while EVI is more sensitive in such cases (Huete et al., 2002).

For the model development, time series of NDVI, EVI and LST at each FLUXNET site were obtained from MODIS Land Product Subsets (<http://daac.ornl.gov/MODIS/modis.html>) (ORNL DAAC, Oak Ridge, Tennessee, USA, last accessed December 2014) for the years when ET data was available since 2000 (see "Period" column in Table 1). NDVI and EVI time series were smoothed using local weighted scatterplot technique (LOWESS) as in Helman et al. (2014a, b) and Helman and Lensky (2015). For model implementation, tiles h20v05, h21v05, h20v06 and h21v06 of the MOD13Q1 product were downloaded for 2000–2014 using the USGS EarthExplorer tool (<http://earthexplorer.usgs.gov>). These tiles fully cover the Eastern Mediterranean region.

Model results were compared with two satellite operational ET products from MODIS (MOD16) and MSG (LSA-SAF MSG ETa) in 2011 at 148 main basins in the Eastern Mediterranean. MODIS and MSG ET products are based on different physical models, and have different spatial and temporal resolutions (1 km/8 days for MODIS, and

Annual ET retrieved solely from satellites' VIs for the EM

D. Helman et al.

Title Page

Abstract

Introduction

Conclusions

References

Tables

Figures

◀

▶

◀

▶

Back

Close

Full Screen / Esc

Printer-friendly Version

Interactive Discussion



3.1 km/30 min and daily for MSG) (Hu et al., 2015). Daily LSA-SAF MSG ETa images were aggregated to one year (365 days for 2011) for North Africa tile (NAfr). The total annual ET MODIS product (MOD16A3) was downloaded for the same tiles of the VIs product. The basins layer map was taken from HydroSHEDS, a mapping product based on high-resolution elevation developed by the Conservation Science Program of World Wildlife Fund (<http://hydrosheds.cr.usgs.gov>). Only main basins with an area greater than 10 km² were selected (Fig. S1 in the Supplement).

3 Methods

3.1 Sites selection

Perennial and annual vegetation in Mediterranean regions have distinctive phenology contributing differently to the VIs signal (Karnieli, 2003; Lu et al., 2003). Helman and Lensky (2015) suggested that to use VIs for ET assessment vegetation systems comprising both annual and perennial vegetation (i.e., forests, woodlands, savannah and shrublands, hereafter PA) should be treated separately from those with only annual vegetation (i.e., croplands and grasslands, hereafter AN).

They found that annual vegetation in the understory of PA systems might contribute significantly to VIs while having very small contribution to total ecosystem ET (Helman and Lensky, 2015). In some cases this results in an apparent phase shift between ET and VIs (Fig. 1) leading to negative or no correlations. Moreover, AN systems showed one singular ET–VI relationship under wide range of rainfall conditions while significantly differ for similar PA systems under different climatic regimes (Helman and Lensky, 2015).

Therefore, we examined ET–VIs relationships in AN and PA systems separately. FLUXNET sites in AN systems were selected from wide range of climatic regimes. FLUXNET sites in PA systems were selected only from Mediterranean-climate regions. Selection of FLUXNET sites had to fulfil the following criteria: (1) at least three years

Annual ET retrieved solely from satellites' VIs for the EM

D. Helman et al.

Title Page

Abstract

Introduction

Conclusions

References

Tables

Figures



Back

Close

Full Screen / Esc

Printer-friendly Version

Interactive Discussion



Annual ET retrieved solely from satellites' VIs for the EM

D. Helman et al.

[Title Page](#)[Abstract](#)[Introduction](#)[Conclusions](#)[References](#)[Tables](#)[Figures](#)[Back](#)[Close](#)[Full Screen / Esc](#)[Printer-friendly Version](#)[Interactive Discussion](#)

of satellite and eddy covariance data in the FLUXNET site, (2) missing data less than 30 days yr^{-1} for ET and 15 % for VIs; and (3) homogeneous vegetation cover near the FLUXNET tower within at least the 250 m spatial resolution of MODIS VIs products. The last criterion was manually assured using Google Earth™. These led us to select 16 FLUXNET sites that represent a wide range of plant functional types and annual ET rates (Table 1).

3.2 Empirical ET models using VIs and LST

Three regression models using VIs and/or LST and ET from eddy covariance towers were tested:

1. Simple regressions between VIs and ET or LST and ET using 16 day or annual data.
2. Multiple regressions using VIs and LST as dependent variables with 16 day or annual data.
3. Modified version of the Temperature and Greenness (TG) model proposed by Sims et al. (2008) using LST as a proxy for radiation and reference ET (Maeda et al., 2011) with 16 day data alone.

We used all models with 16 day ET averages and 16 day VIs/LST data but only the first two models with total annual ET and mean annual VIs/LST because the TG model was designed for 16 day data alone (Sims et al., 2008). In AN we used the integral over the VIs growth season (i.e. after subtracting the annual minimum VIs) instead of the original 16 day VIs data (see in Helman et al., 2014a, b). The integral over the VIs growth season was used in the two regression models against total annual ET (Helman and Lensky, 2015). Multiple regression models were applied only with NDVI and LST or EVI and LST, but not with NDVI and EVI because NDVI and EVI were highly correlated ($R > 0.95$, $p < 0.001$).

The original TG model is based on the correlations between MODIS-EVI and GPP, which are further refined by incorporating LST (Sims et al., 2008):

$$GPP = a \times EVI_{\text{scaled}} \times LST_{\text{scaled}}, \quad (3)$$

where EVI_{scaled} is the scaled EVI set to zero at $EVI = 0.1$ (i.e. $EVI_{\text{scaled}} = EVI - 0.1$) due to absence of photosynthetic activity at this value (Sims et al., 2006); a is the slope of the relationship that enables parameterization of the model; and LST_{scaled} is daytime LST scaled to 1 at an optimum temperature for leaf photosynthetic response around 30°C , decreasing towards 0 at lower and higher temperatures as follows (Sims et al., 2008):

$$LST_{\text{scaled}} = \min \left[\left(\frac{LST}{30} \right); (2.5 - 0.05 \times LST) \right], \quad (4)$$

Note that LST_{scaled} in Eq. (4) is negative at LST higher than 50°C . In such case, LST_{scaled} is set to 0 assuming no photosynthetic activity at those high temperatures following a stomata closure (Sims et al., 2008).

Here, we modified the TG model by using ET instead of GPP in Eq. (3):

$$ET = a \times EVI_{\text{scaled}} \times LST_{\text{scaled}}. \quad (5)$$

The rationale is that GPP and ET are correlated through trade-offs between carbon gains and water loss during photosynthesis processes. We used the modified TG model with EVI and NDVI alternatively in Eq. (5).

3.3 Models evaluation

Pearson's correlation coefficient (R) and mean absolute error (MAE) were used to evaluate the VIs-based ET models. Best models were considered as those with high $|R|$ and low MAE (i.e. lower than the eddy covariance accuracy $\sim 30\%$). A two-tailed student

Annual ET retrieved solely from satellites' VIs for the EM

D. Helman et al.

| | |
|--------------------------|--------------|
| Title Page | |
| Abstract | Introduction |
| Conclusions | References |
| Tables | Figures |
| ◀ | ▶ |
| ◀ | ▶ |
| Back | Close |
| Full Screen / Esc | |
| Printer-friendly Version | |
| Interactive Discussion | |



t test was conducted to examine statistical differences between the models (*p* value). The best model was selected using a performance-simplicity criterion, i.e. the model with the highest *R* (and mean relative error < 30 %) with respect to its complexity (number of variables and operations needed) was preferred.

3.4 Land cover map for model implementation

ET was assessed for the Eastern Mediterranean using the best models for AN and PA systems separately. To produce the required land cover map, we classified pixels as AN/PA based on their NDVI during the year. Low NDVI during the dry season (< 0.25) implies absent or dry vegetation typical for AN systems (Lu et al., 2003). Yet, some PA systems (e.g. open shrublands) also have low NDVI during this period but differ from AN systems by smaller NDVI change (< 0.4) during the growth season (Lu et al., 2003; Roderick et al., 1999).

Hence, we classified pixels with minimum NDVI < 0.25 as AN only if their NDVI increased by more than 0.4 during the growth season. To account for the high NDVI in agricultural fields of the Nile delta, pixels with minimum NDVI smaller or equal to 0.35 were also classified as AN only if their NDVI increased by more than 0.35. All remaining pixels were automatically classified as PA (Fig. S2).

Although this classification procedure is a bit coarse, we preferred it upon the MODIS land cover product for two reasons. First, a significant discrepancy was found between MODIS-based land cover product and actual land cover type distribution in the Eastern Mediterranean (Sprintsin et al., 2009a). Second, this procedure produces a mask at the spatial resolution of the model (250 m), while the MODIS-derived land cover product is available at coarser resolution (500 m).

The produced AN/PA land cover map showed the general pattern known for this region (Fig. S2). Moreover, the total AN area estimated for Israel not considering the Golan Heights grasslands (i.e. considering mostly Israel's croplands) was 255×10^3 ha. This agreed well with the total cropland area reported by the Israeli Central Bureau of Statistics for the same years (220×10^3 ha, CBS 2014).

Annual ET retrieved solely from satellites' Vis for the EM

D. Helman et al.

Title Page

Abstract

Introduction

Conclusions

References

Tables

Figures



Back

Close

Full Screen / Esc

Printer-friendly Version

Interactive Discussion



3.5 Evapotranspiration calculated from water catchments balances

We evaluated our model with mean annual ET calculated from six water catchments balances along gradient rainfall (130–800 mm yr⁻¹) in the Eastern Mediterranean (Fig. S3). The calculation followed the classical water balance equation:

$$ET = P - Q - \frac{dS}{dt}, \quad (6)$$

where P and Q are the total annual precipitation and discharge measured in the catchment, and dS/dt is the change in water storage. For timescales of several years, dS/dt is assumed to be negligible, so the mean annual ET could be simply calculated from P minus Q (Conradt et al., 2013). Because we used water balances averaged over 14 years (i.e. 2000–2013), this assumption was also valid in our case (Table 2).

The water balances approach has some drawbacks like the difficulty to properly estimate precipitation distribution over the catchment and uncertainties about catchment boundaries (Conradt et al., 2013). However, it is the best existing approach to compare in situ ET with satellite-derived ET at a basin scale.

4 Results and discussion

4.1 ET-VIs in systems comprising annual and perennial vegetation

Total annual ET was highly correlated with mean annual NDVI in FLUXNET sites of PA systems with an R ranging from 0.85 to 0.93 (Table 3; Fig. 2). In contrast, 16 day ET averages were only poorly correlated with 16 day NDVI ($R = 0.17$ – 0.63). The same was for total annual ET and mean annual EVI with R of 0.66–0.94 compared to R of 0.28–0.70 when using 16 day EVI and ET data. In average, correlations between total annual ET and mean annual VIs in PA were better by 60% (for ET–NDVI) and 40% (for ET–EVI) from those between 16 day ET and VIs data. The year-to-year changes in

Title Page

Abstract

Introduction

Conclusions

References

Tables

Figures



Back

Close

Full Screen / Esc

Printer-friendly Version

Interactive Discussion



mean annual NDVI and EVI were significant enough to detect even small interannual changes in ET of 20–40 mm yr⁻¹ (e.g. ES-Amo in Fig. 2).

LST was negatively correlated with 16 day and total annual ET in all PA FLUXNET sites. This implies the role of transpiration in attenuating thermal load (Rotem-Mindali et al., 2015). Mean annual LST was highly correlated with total annual ET ($|R| > 0.84$, $p < 0.05$) particularly in sites with low canopy cover (IL-Yat – 30–45 % and ES-LMa – 20–30 %; Casals et al., 2009; Sprintsin et al., 2009b). Those sites had relatively high interannual variability in LST (2–3.5 °C; Fig. 2).

When using all data from PA FLUXNET sites together, correlation coefficients were high as in site-specific annual regressions (Fig. 3). Correlations were high using linear and exponential functions ($R = 0.94$, $p < 0.05$ for both VIs and functions). Mean annual NDVI and EVI explained 71 and 88 % of the variability in total annual ET, which is within the accuracy of the eddy covariance technique for estimating ET (Glenn et al., 2010; Kalma et al., 2008). Annual ET and LST were also correlated through a negative relationship when using all PA together ($R = -0.89$, $p < 0.05$, Fig. 3).

The contribution of annual and perennial vegetation to VIs at the sub pixel level is most difficult to distinguish in PA systems (Karnieli, 2003). In some cases, one of those components might have dominant contribution to VIs but insignificant to the ecosystem flux exchange (Fig. 1). This is probably one of the reasons that VIs could not be used to assess ET at a seasonal timescale (i.e. using 16 day data) in such systems (Helman and Lensky, 2015). However, at interannual timescales (i.e. using the annual mean) relationships between ET and VIs were strong and might be used to retrieve total annual ET in PA systems.

4.2 Comparison between empirical VIs-based ET models

In AN, correlation coefficients from simple regressions of annual ET against VIs growing season integrals using all-sites data were comparable to those when using 16 day data (Table 4). The R from simple regression of 16 day ET against NDVI and EVI was 0.86 for both indices. The R for simple regressions of total annual ET against NDVI

Annual ET retrieved solely from satellites' VIs for the EM

D. Helman et al.

Title Page

Abstract

Introduction

Conclusions

References

Tables

Figures



Back

Close

Full Screen / Esc

Printer-friendly Version

Interactive Discussion



Annual ET retrieved solely from satellites' VIs for the EM

D. Helman et al.

Title Page

Abstract

Introduction

Conclusions

References

Tables

Figures



Back

Close

Full Screen / Esc

Printer-friendly Version

Interactive Discussion



integrals was higher ($R = 0.88$) than that against EVI integrals ($R = 0.79$). However, mean relative error (i.e. MAE/mean) was much lower for annual correlations (12–16 %) than for 16 day correlations (32–33 %, Table 5). The relatively high R for the 16 day ET–VIs regressions in AN supports the biomass-ET–VIs relationship in those systems described elsewhere (Glenn et al., 2010; Helman and Lensky, 2015).

Correlations did not significantly improve ($p > 0.1$) for AN when LST was added in multiple regression models (Table 4 and 5). The R using 16 day data in multiple regression models was 0.87 (for LST with NDVI or EVI) compared to an R of 0.86 for simple regression model (for NDVI or EVI). For the annual data, R was 0.89 and 0.79 (for LST with NDVI or EVI) compared to 0.87 and 0.82 (for LST with NDVI or EVI) from the simple regression model.

In PA, correlations using 16 day data substantially improved ($p < 0.05$ for both indices) for multiple regression model compared to simple regression model with R of 0.71 and 0.73 (for LST with NDVI or EVI) compared to 0.51 and 0.61 (NDVI and EVI). But, R from simple and multiple regression models using annual data were not statistically different ($p > 0.1$). In this case, R from both models was high ($R = 0.94$ and 0.96 for LST with NDVI or EVI, $R = 0.94$ for both ET–NDVI and ET–EVI).

The modified TG model resulted in significantly higher R ($p < 0.05$ for both indices) only for PA and for 16 day data alone ($R = 0.80$ and 0.78 using NDVI or EVI in Eq. 5). However, it was still significantly lower ($p < 0.05$ for both VIs) than simple ET–VIs correlations when using annual data (Table 4 and Fig. S4b). In AN, R from TG and 16 day ET–VIs were not significantly different ($p > 0.1$, Table 4 and Fig. S4a).

4.3 PaVI-E model

NDVI and EVI were the best explanatory factors of the interannual change in ET at both, AN and PA systems (Table 4). This means that simple ET–VIs regression functions could be used to estimate total annual ET in those systems (Helman and Lensky, 2015). Multiple regression and TG modified models had higher R and lower MAE in some cases (Table 5), but differences were not significant ($p > 0.05$). Hence, we chose

the simple regression function as the best model following the performance-simplicity criterion. The functions obtained from ET–NDVI and ET–EVI regressions were averaged for PA:

$$ET_{\text{Annual}} = [85 \exp(3\text{NDVI}) + 65 \exp(6.9\text{EVI})]/2, \quad (7)$$

5 and AN systems:.

$$ET_{\text{Annual}} = [187 \exp(0.23\text{NDVI}_{\text{GSI}}) + 224 \exp(0.26\text{EVI}_{\text{GSI}})]/2. \quad (8)$$

Where ET_{Annual} is the total annual ET in mm yr^{-1} . NDVI and EVI in Eq. (7) are the mean annual NDVI and EVI. NDVI_{GSI} and EVI_{GSI} in Eq. (8) are the integrals over NDVI and EVI growth season, respectively. The exponential function was preferred over the linear one because the latter leads to negative values at NDVI (and EVI) of ~ 0.1 (a value that usually corresponds to soil background), while in reality ET is still greater than zero due to surface evaporation (Helman and Lensky, 2015).

Finally, we named this model PaVI-E, the Parameterization of Vegetation Indices for ET estimation model. The mean relative error of PaVI-E was 13 and 12% for AN and PA, respectively. This is within the accuracy of the eddy covariance measurements that were used for calibration and much lower than the reported from complex models (Glenn et al., 2010; Kalma et al., 2008). PaVI-E was used to assess total annual ET at spatial resolution of 250 m for the Eastern Mediterranean after using the land cover map created for AN and PA as a mask (Sect. 3.3 and Fig. S2).

20 **4.4 Model evaluation in the Eastern Mediterranean**

4.4.1 Comparison with MODIS and MSG ET products

ET estimates from PaVI-E were compared with two operational remote sensing ET products in 148 large basins ($> 10 \text{ km}^2$). The spatial patterns of annual ET for 2011 from PaVI-E, MOD16 and MSG were generally similar over the EM (Fig. 4). The three

Annual ET retrieved solely from satellites' Vis for the EM

D. Helman et al.

Title Page

Abstract

Introduction

Conclusions

References

Tables

Figures



Back

Close

Full Screen / Esc

Printer-friendly Version

Interactive Discussion



models show a general west to east and south to north ET gradients along the eastern coastline, matching the rainfall gradients of this region (Ziv et al., 2014). Also, all three models show higher ET estimates over agricultural fields in the Nile delta compared to the surrounding desert.

5 However, some discrepancies also exist. MOD16 estimates were lower along the EM coast compared to PaVI-E and MSG. ET estimates from MSG were relatively high along the eastern coast especially to the east of the Sea of Galilee (mean ET of $\sim 800 \text{ mm yr}^{-1}$). Differences between models were particularly noted over the Nile delta. The average annual ET over the Nile delta for 2011 was 160 mm yr^{-1} from MSG, 10 530 mm yr^{-1} from MOD16, and 680 mm yr^{-1} from PaVI-E. While MSG estimates seem extremely low for such highly productive area, PaVI-E and MOD16 estimates agreed well with the high ET reported from in situ measurements (Elhag et al., 2011). Besides the advantage of an improved spatial resolution (250 m compared to 1 and 3.1 km of MOD16 and MSG) PaVI-E also has the ability to produce spatially continuous ET compared to MSG and MODIS products (Fig. 4).

15 Comparing the three models at a basin scale resulted in good agreement between them ($R = 0.77$ and 0.75 for PaVI-E vs. MOD16 and MSG, respectively, $p < 0.001$ for both; Fig. 5). MOD16 and MSG products had small bias with respect to PaVI-E with a relative bias (i.e. bias/mean) of -5.2 and 5.2% and slopes of 0.76 and 1.17 for MOD16 and MSG ET products, respectively.

20 The relatively higher/lower MOD16 estimates in xeric/mesic Mediterranean areas (Fig. 5) was already pointed out by Trambauer et al. (2014) that compared this product with several independent ET models. Furthermore, comparison of MOD16 and MSG ET products in Europe showed that correlations with in situ ET (from 15-eddy covariance sites) were better for MSG (Hu et al., 2015), and that MOD16 underestimate ET 25 in Mediterranean dry regions similarly to the observed in this study (Fig. 4).

Annual ET retrieved solely from satellites' Vis for the EM

D. Helman et al.

[Title Page](#)[Abstract](#)[Introduction](#)[Conclusions](#)[References](#)[Tables](#)[Figures](#)[Back](#)[Close](#)[Full Screen / Esc](#)[Printer-friendly Version](#)[Interactive Discussion](#)

4.4.2 Evaluation against ET from water balances along rainfall gradient

ET estimates from PaVI-E were evaluated against ET calculated from six water catchments along rainfall gradient in the Eastern Mediterranean (EM). PaVI-E estimates were highly correlated with ET from water balances ($R = 0.92$, $p < 0.01$) at six catchments along the north–south rainfall gradient in the EM (Fig. 6a). ET from MOD16 and MSG were also significantly correlated with the water balances-derived ET ($p < 0.05$, Fig. S5). All three models had very similar ET estimates in the mountain aquifer catchments (MA-N, MA-CS, and MA-S), lower than the calculated from water balances (Fig. 6b). Still, within the accuracy of the models ($\sim 12\%$) and gauging/rainfall distribution uncertainties ($\sim 10\text{--}15\%$, Conradt et al., 2013).

As shown in Fig. 4, ET estimates derived from PaVI-E are significantly higher than those from MOD16 and MSG in the dry areas of the EM. This is due to the exponential functions used in PaVI-E (Eqs. 7 and 8). It generated a comparable ET to that calculated from water balances at the dry catchment of Mamashit with a slight overestimation (15%) of PaVI-E (Fig. 6b). MSG largely underestimated the calculated ET in Mamashit (by more than 85%) while MOD16 had no data for this area.

5 Conclusions

Three VIs-based ET models using only eddy covariance ET and MODIS vegetation indices and land surface temperature data were tested. Vegetation systems comprising mostly annual vegetation (i.e., grasslands and croplands) had strong VIs relationships with intra-annual (16 day ET averages) and interannual (total annual ET) ET estimates. Yet, the mean relative error was larger for intra-annual relationships compared to interannual relationships (32% compared to 12%). In systems with annual and perennial vegetation (i.e., forests, woodlands, savannah and shrublands) ET–VIs relationships were strong only at interannual timescales (i.e. using annual data). Multiple regression

Annual ET retrieved solely from satellites' VIs for the EM

D. Helman et al.

Title Page

Abstract

Introduction

Conclusions

References

Tables

Figures



Back

Close

Full Screen / Esc

Printer-friendly Version

Interactive Discussion



and modified TG models using VIs and LST were not significantly better than simple ET–VIs regression models in both vegetation systems ($p > 0.1$).

Following a performance-simplicity criterion we used the simple ET–VIs interannual relationships to retrieve total annual ET for the Eastern Mediterranean. This model named here the parameterized vegetation index for ET estimates model (PaVI-E) had comparable estimates to those from MODIS and MSG ET products in the Eastern Mediterranean. Models' estimates also agreed well with ET calculated from six water catchments balances along the south–north EM rainfall gradient. The advantage of PaVI-E is in its simplicity and resolution (250 m) compared to the coarser resolutions of MODIS and MSG ET products (1 and 3.1 km, respectively).

Improvement in the estimation of ET is essential for water budget calculations and water resource management especially in water limited regions. Here we propose the use of a simple model to retrieve annual ET at 250 m spatial resolution suitable for the Eastern Mediterranean region. We are confident that using PaVI-E will enhance the hydrological study in this region where ET plays a major role in the hydrological cycle.

The Supplement related to this article is available online at [doi:10.5194/acpd-15-15397-2015-supplement](https://doi.org/10.5194/acpd-15-15397-2015-supplement).

Acknowledgements. Authors are grateful to the Rieger Foundation, USA and the Israeli Hydrological Service, Water Authority (IWA) for supporting David Helman in his research. Also thanks to Shilo Shiff for his assistance with the LSA-SAF MSG hdf files. This research was supported by the IWA (Grant No. 4500962964). This study used eddy covariance data acquired by the FLUXNET community and in particular by the following networks: AmeriFlux (U.S. Department of Energy, Biological and Environmental Research, Terrestrial Carbon Program), CarboItaly and CarboEuropeIP. MODIS subsets and tiles land products were acquired from the Oak Ridge National Laboratory Distributed Active Archive Centre (ORNL DAAC) and the U.S. Geological Survey (USGS).

Annual ET retrieved solely from satellites' VIs for the EM

D. Helman et al.

| | |
|--------------------------|--------------|
| Title Page | |
| Abstract | Introduction |
| Conclusions | References |
| Tables | Figures |
| ◀ | ▶ |
| ◀ | ▶ |
| Back | Close |
| Full Screen / Esc | |
| Printer-friendly Version | |
| Interactive Discussion | |



References

- Anderson, M. C., Norman, J. M., Kustas, W. P., Houborg, R., Starks, P. J., and Agam, N.: A thermal-based remote sensing technique for routine mapping of land-surface carbon, water and energy fluxes from field to regional scales, *Remote Sens. Environ.*, 112, 4227–4241, doi:10.1016/j.rse.2008.07.009, 2008.
- Baldocchi, D. D., Xu, L., and Kiang, N.: How plant functional-type, weather, seasonal drought, and soil physical properties alter water and energy fluxes of an oak–grass savanna and an annual grassland, *Agr. Forest Meteorol.*, 123, 13–39, doi:10.1016/j.agrformet.2003.11.006, 2004.
- Casals, P., Gimeno, C., Carrara, A., Lopez-Sangil, L., and Sanz, M.: Soil CO₂ efflux and extractable organic carbon fractions under simulated precipitation events in a Mediterranean Dehesa, *Soil Biol. Biochem.*, 41, 1915–1922, doi:10.1016/j.soilbio.2009.06.015, 2009.
- Chamizo, S., Cantón, Y., Miralles, I., and Domingo, F.: Biological soil crust development affects physicochemical characteristics of soil surface in semiarid ecosystems, *Soil Biol. Biochem.*, 49, 96–105, doi:10.1016/j.soilbio.2012.02.017, 2012.
- Chen, X., Su, Z., Ma, Y., Liu, S., Yu, Q., and Xu, Z.: Development of a 10-year (2001–2010) 0.1° data set of land-surface energy balance for mainland China, *Atmos. Chem. Phys.*, 14, 13097–13117, doi:10.5194/acp-14-13097-2014, 2014.
- Colaizzi, P. D., Kustas, W. P., Anderson, M. C., Agam, N., Tolck, J. A., Evett, S. R., Howell, T. A., Gowda, P. H., and O’Shaughnessy, S. A.: Two-source energy balance model estimates of evapotranspiration using component and composite surface temperatures, *Adv. Water Resour.*, 50, 134–151, doi:10.1016/j.advwatres.2012.06.004, 2012.
- Conradt, T., Wechsung, F., and Bronstert, A.: Three perceptions of the evapotranspiration landscape: comparing spatial patterns from a distributed hydrological model, remotely sensed surface temperatures, and sub-basin water balances, *Hydrol. Earth Syst. Sci.*, 17, 2947–2966, doi:10.5194/hess-17-2947-2013, 2013.
- Craine, J. M., Nippert, J. B., Elmore, A. J., Skibbe, A. M., Hutchinson, S. L., and Brunsell, N. A.: Timing of climate variability and grassland productivity, *P. Natl. Acad. Sci. USA*, 109, 3401–3405, 2012.
- Elhag, M., Psilovikos, A., Manakos, I., and Perakis, K.: Application of the SEBS water balance model in estimating daily evapotranspiration and evaporative fraction from remote sensing

Annual ET retrieved solely from satellites’ Vis for the EM

D. Helman et al.

Title Page

Abstract

Introduction

Conclusions

References

Tables

Figures



Back

Close

Full Screen / Esc

Printer-friendly Version

Interactive Discussion



Annual ET retrieved solely from satellites' Vis for the EM

D. Helman et al.

Title Page

Abstract

Introduction

Conclusions

References

Tables

Figures



Back

Close

Full Screen / Esc

Printer-friendly Version

Interactive Discussion



data over the Nile delta, *Water Resour. Manag.*, 25, 2731–2742, doi:10.1007/s11269-011-9835-9, 2011.

Glenn, E., Nagler, P., and Huete, A.: Vegetation index methods for estimating evapotranspiration by remote sensing, *Surv. Geophys.*, 31, 531–555, doi:10.1007/s10712-010-9102-2, 2010.

5 Glenn, E. P., Neale, C. M. U., Hunsaker, D. J., and Nagler, P. L.: Vegetation index-based crop coefficients to estimate evapotranspiration by remote sensing in agricultural and natural ecosystems, *Hydrol. Process.*, 25, 4050–4062, doi:10.1002/hyp.8392, 2011.

Helman, D. and Lensky, I. M.: Empirical relationships between evapotranspiration and MODIS vegetation indices in grasslands, croplands and evergreen forests, *Agr. Forest Meteorol.*, in review, 2015.

10 Helman, D., Lensky, I. M., Mussery, A., and Leu, S.: Rehabilitating degraded drylands by creating woodland islets: assessing long-term effects on aboveground productivity and soil fertility, *Agr. Forest Meteorol.*, 195–196, 52–60, doi:10.1016/j.agrformet.2014.05.003, 2014a.

Helman, D., Mussery, A., Lensky, I. M., and Leu, S.: Detecting changes in biomass productivity in a different land management regimes in drylands using satellite-derived vegetation index, *Soil Use Manage.*, 30, 32–39, doi:10.1111/sum.12099, 2014b.

15 Hollinger, S. E., Bernacchi, C. J., and Meyers, T. P.: Carbon budget of mature no-till ecosystem in North Central Region of the United States, *Agr. Forest Meteorol.*, 130, 59–69, doi:10.1016/j.agrformet.2005.01.005, 2005.

20 Hu, G., Jia, L., and Menenti, M.: Comparison of MOD16 and LSA-SAF MSG evapotranspiration products over Europe for 2011, *Remote Sens. Environ.*, 156, 510–526, doi:10.1016/j.rse.2014.10.017, 2015.

Huete, A., Didan, K., Miura, T., Rodriguez, E. P., Gao, X., and Ferreira, L. G.: Overview of the radiometric and biophysical performance of the MODIS vegetation indices, *Remote Sens. Environ.*, 83, 195–213, 2002.

25 Jung, M., Reichstein, M., and Bondeau, A.: Towards global empirical upscaling of FLUXNET eddy covariance observations: validation of a model tree ensemble approach using a biosphere model, *Biogeosciences*, 6, 2001–2013, doi:10.5194/bg-6-2001-2009, 2009.

30 Jung, M., Reichstein, M., Ciais, P., Seneviratne, S. I., Sheffield, J., Goulden, M. L., Bonan, G., Cescatti, A., Chen, J., de Jeu, R., Dolman, A. J., Eugster, W., Gerten, D., Gianelle, D., Gobron, N., Heinke, J., Kimball, J., Law, B. E., Montagnani, L., Mu, Q., Mueller, B., Oleson, K., Papale, D., Richardson, A. D., Rouspard, O., Running, S., Tomelleri, E., Viovy, N., Weber, U., Williams, C., Wood, E., Zaehle, S., and Zhang, K.: Recent decline in the

Annual ET retrieved solely from satellites' Vis for the EM

D. Helman et al.

Title Page

Abstract

Introduction

Conclusions

References

Tables

Figures



Back

Close

Full Screen / Esc

Printer-friendly Version

Interactive Discussion



global land evapotranspiration trend due to limited moisture supply, *Nature*, 467, 951–954, doi:10.1038/nature09396, 2010.

Kalma, J., McVicar, T., and McCabe, M.: Estimating land surface evaporation: a review of methods using remotely sensed surface temperature data, *Surv. Geophys.*, 29, 421–469, doi:10.1007/s10712-008-9037-z, 2008.

Karnieli, A.: Natural vegetation phenology assessment by ground spectral measurements in two semi-arid environments, *Int. J. Biometeorol.*, 47, 179–187, doi:10.1007/s00484-003-0169-z, 2003.

Kutsch, W. L., Aubinet, M., Buchmann, N., Smith, P., Osborne, B., Eugster, W., Wattenbach, M., Schrupf, M., Schulze, E. D., Tomelleri, E., Ceschia, E., Bernhofer, C., Béziat, P., Carrara, A., Di Tommasi, P., Grünwald, T., Jones, M., Magliulo, V., Marloie, O., Moureaux, C., Olioso, A., Sanz, M. J., Saunders, M., Søgaard, H., and Ziegler, W.: The net biome production of full crop rotations in Europe, *Agr. Ecosyst. Environ.*, 139, 336–345, doi:10.1016/j.agee.2010.07.016, 2010.

Lu, H., Raupach, M. R., McVicar, T. R., and Barrett, D. J.: Decomposition of vegetation cover into woody and herbaceous components using AVHRR NDVI time series, *Remote Sens. Environ.*, 86, 1–18, doi:10.1016/S0034-4257(03)00054-3, 2003.

Ma, Y., Zhu, Z., Zhong, L., Wang, B., Han, C., Wang, Z., Wang, Y., Lu, L., Amatya, P. M., Ma, W., and Hu, Z.: Combining MODIS, AVHRR and in situ data for evapotranspiration estimation over heterogeneous landscape of the Tibetan Plateau, *Atmos. Chem. Phys.*, 14, 1507–1515, doi:10.5194/acp-14-1507-2014, 2014.

Maeda, E. E., Wiberg, D. A., and Pellikka, P. K. E.: Estimating reference evapotranspiration using remote sensing and empirical models in a region with limited ground data availability in Kenya, *Appl. Geogr.*, 31, 251–258, doi:10.1016/j.apgeog.2010.05.011, 2011.

Maselli, F., Papale, D., Chiesi, M., Matteucci, G., Angeli, L., Raschi, A., and Seufert, G.: Operational monitoring of daily evapotranspiration by the combination of MODIS NDVI and ground meteorological data: application and evaluation in Central Italy, *Remote Sens. Environ.*, 152, 279–290, doi:10.1016/j.rse.2014.06.021, 2014.

Maseyk, K. S., Lin, T., Rotenberg, E., Grünzweig, J. M., Schwartz, A., and Yakir, D.: Physiology–phenology interactions in a productive semi-arid pine forest, *New Phytol.*, 178, 603–616, 2008.

Moffat, A. M., Papale, D., Reichstein, M., Hollinger, D. Y., Richardson, A. D., Barr, A. G., Beckstein, C., Braswell, B. H., Churkina, G., and Desai, A. R.: Comprehensive comparison of gap-

Annual ET retrieved solely from satellites' Vis for the EM

D. Helman et al.

Title Page

Abstract

Introduction

Conclusions

References

Tables

Figures



Back

Close

Full Screen / Esc

Printer-friendly Version

Interactive Discussion



filling techniques for eddy covariance net carbon fluxes, *Agr. Forest Meteorol.*, 147, 209–232, 2007.

Nagler, P. L., Brown, T., Hultine, K. R., van Riper III, C., Bean, D. W., Dennison, P. E., Murray, R. S., and Glenn, E. P.: Regional scale impacts of Tamarix leaf beetles (*Diorhabda carinulata*) on the water availability of western U. S. rivers as determined by multi-scale remote sensing methods, *Remote Sens. Environ.*, 118, 227–240, doi:10.1016/j.rse.2011.11.011, 2012.

Oki, T. and Kanae, S.: Global hydrological cycles and world water resources, *Science*, 313, 1068–1072, 2006.

Reichstein, M., Falge, E., Baldocchi, D., Papale, D., Aubinet, M., Berbigier, P., Bernhofer, C., Buchmann, N., Gilmanov, T., Granier, A., Grünwald, T., Havránková, K., Ilvesniemi, H., Janous, D., Knohl, A., Laurila, T., Lohila, A., Loustau, D., Matteucci, G., Meyers, T., Miglietta, F., Ourcival, J.-M., Pumpanen, J., Rambal, S., Rotenberg, E., Sanz, M., Tenhunen, J., Seufert, G., Vaccari, F., Vesala, T., Yakir, D., and Valentini, R.: On the separation of net ecosystem exchange into assimilation and ecosystem respiration: review and improved algorithm, *Glob. Change Biol.*, 11, 1424–1439, doi:10.1111/j.1365-2486.2005.001002.x, 2005.

Reichstein, M., Ciais, P., Papale, D., Valentini, R., Running, S., Viovy, N., Cramer, W., Granier, A., Ogee, J., Allard, V., Aubinet, M., Bernhofer, C., Buchmann, N., Carrara, A., Grunwald, T., Heimann, M., Heinesch, B., Knohl, A., Kutsch, W., Loustau, D., Manca, G., Matteucci, G., Miglietta, F., Ourcival, J. M., Pilegaard, K., Pumpanen, J., Rambal, S., Schaphoff, S., Seufert, G., Soussana, J.-F., Sanz, M.-J., Vesala, T., and Zhao, M.: Reduction of ecosystem productivity and respiration during the European summer 2003 climate anomaly: a joint flux tower, remote sensing and modelling analysis, *Glob. Change Biol.*, 13, 634–651, doi:10.1111/j.1365-2486.2006.01224.x, 2007.

Roderick, M. L., Noble, I. R., and Cridland, S. W.: Estimating woody and herbaceous vegetation cover from time series satellite observations, *Global Ecol. Biogeogr.*, 8, 501–508, doi:10.1046/j.1365-2699.1999.00153.x, 1999.

Rotem-Mindali, O., Michael, Y., Helman, D., and Lensky, I. M.: The role of local land-use on the urban heat island effect of Tel Aviv as assessed from satellite remote sensing, *Appl. Geogr.*, 56, 145–153, doi:10.1016/j.apgeog.2014.11.023, 2015.

Rouse, J. W., Haas, R. H., and Schell, J. A.: Monitoring the vernal advancement and retrogradation (greenwave effect) of natural vegetation, Texas A and M University, College Station, 1974.

Annual ET retrieved solely from satellites' Vis for the EM

D. Helman et al.

Title Page

Abstract

Introduction

Conclusions

References

Tables

Figures



Back

Close

Full Screen / Esc

Printer-friendly Version

Interactive Discussion



Scott, R. L., Hamerlynck, E. P., Jenerette, G. D., Moran, M. S., and Barron-Gafford, G. A.: Carbon dioxide exchange in a semidesert grassland through drought-induced vegetation change, *J. Geophys. Res.*, 115, G03026, doi:10.1029/2010JG001348, 2010.

Senay, G. B., Leake, S., Nagler, P. L., Artan, G., Dickinson, J., Cordova, J. T., and Glenn, E. P.: Estimating basin scale evapotranspiration (ET) by water balance and remote sensing methods, *Hydrol. Process.*, 25, 4037–4049, doi:10.1002/hyp.8379, 2011.

Shi, Q. and Liang, S.: Surface-sensible and latent heat fluxes over the Tibetan Plateau from ground measurements, reanalysis, and satellite data, *Atmos. Chem. Phys.*, 14, 5659–5677, doi:10.5194/acp-14-5659-2014, 2014.

Sims, D. A., Rahman, A. F., Cordova, V. D., El-Masri, B. Z., Baldocchi, D. D., Flanagan, L. B., Goldstein, A. H., Hollinger, D. Y., Misson, L., Monson, R. K., Oechel, W. C., Schmid, H. P., Wofsy, S. C., and Xu, L.: On the use of MODIS EVI to assess gross primary productivity of North American ecosystems, *J. Geophys. Res.*, 111, G04015, doi:10.1029/2006JG000162, 2006.

Sims, D. A., Rahman, A. F., Cordova, V. D., El-Masri, B. Z., Baldocchi, D. D., Bolstad, P. V., Flanagan, L. B., Goldstein, A. H., Hollinger, D. Y., Misson, L., Monson, R. K., Oechel, W. C., Schmid, H. P., Wofsy, S. C., and Xu, L.: A new model of gross primary productivity for North American ecosystems based solely on the enhanced vegetation index and land surface temperature from MODIS, *Remote Sens. Environ.*, 112, 1633–1646, doi:10.1016/j.rse.2007.08.004, 2008.

Skiba, U., Drewer, J., Tang, Y. S., van Dijk, N., Helfter, C., Nemitz, E., Famulari, D., Cape, J. N., Jones, S. K., Twigg, M., Pihlatie, M., Vesala, T., Larsen, K. S., Carter, M. S., Ambus, P., Ibrom, A., Beier, C., Hensen, A., Frumau, A., Erisman, J. W., Brüggemann, N., Gasche, R., Butterbach-Bahl, K., Neftel, A., Spirig, C., Horvath, L., Freibauer, A., Cellier, P., Laville, P., Loubet, B., Magliulo, E., Bertolini, T., Seufert, G., Andersson, M., Manca, G., Laurila, T., Aurela, M., Lohila, A., Zechmeister-Boltenstern, S., Kitzler, B., Schauffler, G., Siemens, J., Kindler, R., Flechard, C., and Sutton, M. A.: Biosphere–atmosphere exchange of reactive nitrogen and greenhouse gases at the NitroEurope core flux measurement sites: measurement strategy and first data sets, *Agr. Ecosyst. Environ.*, 133, 139–149, doi:10.1016/j.agee.2009.05.018, 2009.

Sprintsin, M., Karnieli, A., Berliner, P., Rotenberg, E., Yakir, D., and Cohen, S.: Evaluating the performance of the MODIS Leaf Area Index (LAI) product over a Mediterranean dry-

Annual ET retrieved solely from satellites' Vis for the EM

D. Helman et al.

Title Page

Abstract

Introduction

Conclusions

References

Tables

Figures



Back

Close

Full Screen / Esc

Printer-friendly Version

Interactive Discussion



land planted forest, *Int. J. Remote Sens.*, 30, 5061–5069, doi:10.1080/01431160903032885, 2009a.

Sprintsin, M., Karnieli, A., Sprintsin, S., Cohen, S., and Berliner, P.: Relationships between stand density and canopy structure in a dryland forest as estimated by ground-based measurements and multi-spectral spaceborne images, *J. Arid Environ.*, 73, 955–962, doi:10.1016/j.jaridenv.2009.04.011, 2009b.

Suyker, A. E. and Verma, S. B.: Interannual water vapor and energy exchange in an irrigated maize-based agroecosystem, *Agr. Forest Meteorol.*, 148, 417–427, doi:10.1016/j.agrformet.2007.10.005, 2008.

Tillman, F. D., Callegary, J. B., Nagler, P. L., and Glenn, E. P.: A simple method for estimating basin-scale groundwater discharge by vegetation in the basin and range province of Arizona using remote sensing information and geographic information systems, *J. Arid Environ.*, 82, 44–52, doi:10.1016/j.jaridenv.2012.02.010, 2012.

Trambauer, P., Dutra, E., Maskey, S., Werner, M., Pappenberger, F., van Beek, L. P. H., and Uhlenbrook, S.: Comparison of different evaporation estimates over the African continent, *Hydrol. Earth Syst. Sci.*, 18, 193–212, doi:10.5194/hess-18-193-2014, 2014.

Tsarouchi, G. M., Buytaert, W., and Mijic, A.: Coupling a land-surface model with a crop growth model to improve ET flux estimations in the Upper Ganges basin, India, *Hydrol. Earth Syst. Sci.*, 18, 4223–4238, doi:10.5194/hess-18-4223-2014, 2014.

Wilson, T. B. and Meyers, T. P.: Determining vegetation indices from solar and photosynthetically active radiation fluxes, *Agr. Forest Meteorol.*, 144, 160–179, doi:10.1016/j.agrformet.2007.04.001, 2007.

Zemp, D. C., Schleussner, C.-F., Barbosa, H. M. J., van der Ent, R. J., Donges, J. F., Heinke, J., Sampaio, G., and Rammig, A.: On the importance of cascading moisture recycling in South America, *Atmos. Chem. Phys.*, 14, 13337–13359, doi:10.5194/acp-14-13337-2014, 2014.

Ziv, B., Saaroni, H., Pargament, R., Harpaz, T., and Alpert, P.: Trends in rainfall regime over Israel, 1975–2010, and their relationship to large-scale variability, *Reg. Environ. Change*, 14, 1751–1764, doi:10.1007/s10113-013-0414-x, 2014.

Annual ET retrieved
solely from satellites'
Vis for the EM

D. Helman et al.

Table 1. Description of the 16 selected FLUXNET sites. Horizontal line divides between the six FLUXNET sites in PA systems (Up) and the ten FLUXNET sites in AN systems (Bottom). Plant functional types (PFT) include CSH: closed shrublands, WDL: woodland, SAV: savannah, ENF: evergreen needle-leaved forest, WSA: woody savannah, CRO: croplands, and GRA: grasslands. Mean annual precipitation (P) is in mm yr^{-1} for the years in which ET data was used (Period).

| Site ID | Lat | Lon | PFT | Main species | P | Period | Reference |
|---------|-------|---------|-----|-------------------------|------|-----------|--------------------------|
| ES-Amo | 36.83 | -2.25 | OSH | Dwarf shrubs | 200 | 2009–2011 | Chamizo et al. (2012) |
| IL-Yat | 31.35 | 35.05 | WDL | <i>Pinus halepensis</i> | 300 | 2003–2009 | Maseyk et al. (2008) |
| ES-LMa | 39.94 | -5.77 | SAV | <i>Quercus ilex</i> | 660 | 2004–2009 | Casals et al. (2009) |
| ES-ES | 39.35 | -0.32 | ENF | <i>Pinus halepensis</i> | 580 | 2001–2006 | Reichstein et al. (2007) |
| FR-Lbr | 44.72 | -0.77 | WSA | <i>Pinus pinaster</i> | 825 | 2004–2008 | Reichstein et al. (2007) |
| US-Blo | 38.90 | -120.63 | ENF | <i>Pinus ponderosa</i> | 1350 | 2001–2006 | Sims et al. (2006) |
| ES-ES2 | 39.28 | -0.32 | CRO | Rice | 620 | 2005–2008 | Kutsch et al. (2010) |
| IT-Cas | 45.07 | 8.72 | CRO | Rice | 960 | 2007–2010 | Skiba et al. (2009) |
| US-Bo1 | 40.01 | -88.29 | CRO | Corn–soybeans | 795 | 2001–2006 | Hollinger et al. (2005) |
| US-Ne1 | 41.17 | -96.48 | CRO | Maize | 590 | 2002–2004 | Suyker and Verma (2008) |
| US-Ne2 | 41.16 | -96.47 | CRO | Maize–soybean | 590 | 2002–2004 | Suyker and Verma (2008) |
| US-Ne3 | 41.18 | -96.44 | CRO | Maize–soybean | 590 | 2002–2005 | Suyker and Verma (2008) |
| US-Var | 38.41 | -120.95 | GRA | C3 grass & herbs | 465 | 2003–2009 | Baldocchi et al. (2004) |
| US-Kon | 39.08 | -96.56 | GRA | C4 grasses | 660 | 2007–2012 | Craine et al. (2012) |
| US-Wkg | 31.74 | -109.94 | GRA | C4 grasses | 190 | 2005–2007 | Scott et al. (2010) |
| US-Goo | 34.25 | -89.87 | GRA | C4 grasses | 1300 | 2003–2006 | Wilson and Meyers (2007) |

Title Page

Abstract

Introduction

Conclusions

References

Tables

Figures

◀

▶

◀

▶

Back

Close

Full Screen / Esc

Printer-friendly Version

Interactive Discussion



**Annual ET retrieved
solely from satellites’
Vis for the EM**

D. Helman et al.

Table 2. Water balances from six catchments along the north to south rainfall gradient in the Eastern Mediterranean (Fig. S3). Catchments area is in 10^3 ha. Precipitation (P), discharge (Q) and calculated ET as $P-Q$, are all in mm yr^{-1} . Fluxes were averaged over the years 2000–2013.

| Name | Area | P | Q | ET |
|----------|------|-----|-----|-----|
| Kziv | 13 | 799 | 284 | 515 |
| HaShofet | 1.2 | 654 | 183 | 471 |
| MA-N | 59 | 615 | 193 | 422 |
| MA-CS | 93 | 592 | 202 | 390 |
| MA-S | 28 | 619 | 257 | 362 |
| Mamashit | 6 | 130 | 28 | 102 |

Title Page

Abstract

Introduction

Conclusions

References

Tables

Figures



Back

Close

Full Screen / Esc

Printer-friendly Version

Interactive Discussion



Annual ET retrieved solely from satellites' VIs for the EM

D. Helman et al.

Table 3. Correlations coefficients (R) of 16 day ET averages and 16 day MODIS-derived NDVI, EVI and daytime LST (LST, °C); and of total annual ET and mean annual NDVI, EVI and LST in the 6 FLUXNET sites of PA systems (perennials and annuals vegetation systems, i.e. forests, woodlands, savannah and shrublands).

| Site ID | NDVI | | EVI | | LST | |
|---------|--------|--------|--------|--------|--------|--------|
| | 16 day | Annual | 16 day | Annual | 16 day | Annual |
| ES-Amo | 0.63 | 0.89 | 0.62 | 0.71 | -0.51 | -0.33 |
| IL-Yat | 0.62 | 0.88 | 0.70 | 0.89 | -0.36 | -0.84 |
| ES-LMa | 0.17 | 0.93 | 0.28 | 0.80 | -0.22 | -0.93 |
| ES-ES | 0.41 | 0.91 | 0.30 | 0.94 | -0.62 | -0.32 |
| FR-Lbr | 0.36 | 0.85 | 0.68 | 0.93 | -0.65 | -0.63 |
| US-Blo | 0.17 | 0.92 | 0.46 | 0.66 | -0.87 | -0.59 |

[Title Page](#)
[Abstract](#)
[Introduction](#)
[Conclusions](#)
[References](#)
[Tables](#)
[Figures](#)
[⏪](#)
[⏩](#)
[◀](#)
[▶](#)
[Back](#)
[Close](#)
[Full Screen / Esc](#)
[Printer-friendly Version](#)
[Interactive Discussion](#)


Annual ET retrieved solely from satellites' VIs for the EM

D. Helman et al.

Table 4. Correlations coefficients (R) of three VIs-based ET models using MODIS-derived NDVI, EVI and daytime LST (LST, °C). Results are for models using 16 day/annual data in AN (annual vegetation systems, i.e. croplands and grasslands), and PA (perennials and annuals vegetation systems, i.e. forests, savannah and shrublands) systems. All R were significant at $p < 0.05$ except for the 16 day ET–LST simple regression in PA. Mean annual NDVI and EVI were regressed against total annual ET using linear and exponential functions.

| Model type | Variables used | AN | | PA | |
|---------------------|-----------------------------|--------|--------|--------------------|--------|
| | | 16 day | Annual | 16 day | Annual |
| Simple regression | NDVI (linear) | 0.86 | 0.88 | 0.51 | 0.94 |
| | NDVI (expo) | | 0.87 | | 0.94 |
| | EVI (linear) | 0.86 | 0.79 | 0.61 | 0.95 |
| | EVI (expo) | | 0.82 | | 0.94 |
| | LST | −0.42 | −0.64 | 0.00 ^{ns} | −0.89 |
| Multiple regression | NDVI, LST | 0.87 | 0.89 | 0.71 | 0.94 |
| | EVI, LST | 0.87 | 0.79 | 0.73 | 0.96 |
| Modified TG | NDVI, LST _{scaled} | 0.87 | | 0.78 | |
| | EVI, LST _{scaled} | 0.87 | | 0.80 | |

Title Page

Abstract

Introduction

Conclusions

References

Tables

Figures

◀

▶

◀

▶

Back

Close

Full Screen / Esc

Printer-friendly Version

Interactive Discussion



Annual ET retrieved solely from satellites' Vis for the EM

D. Helman et al.

Table 5. The mean absolute error (MAE) for Table 4. The 16 day MAE is in mm d^{-1} , while annual MAE is in mm yr^{-1} . In parenthesis is the mean relative error (i.e. MAE/mean) in %.

| Model type | Variables used | AN | | PA | |
|---------------------|-----------------------------|-----------|----------|-------------------------|---------|
| | | 16 day | Annual | 16 day | Annual |
| Simple regression | NDVI (linear) | 0.51 (32) | 66 (12) | 0.65 (47) | 52 (11) |
| | NDVI (expo) | | 83 (15) | | 58 (12) |
| | EVI (linear) | 0.52 (33) | 79 (14) | 0.59 (43) | 53 (11) |
| | EVI (expo) | | 90 (16) | | 63 (13) |
| | LST | 0.94 (60) | 119 (21) | 0.78 (57) ^{ns} | 74 (15) |
| Multiple regression | NDVI, LST | 0.51 (32) | 63 (11) | 0.57 (41) | 52 (11) |
| | EVI, LST | 0.51 (33) | 79 (14) | 0.54 (40) | 49 (10) |
| Modified TG | NDVI, LST _{scaled} | 0.48 (30) | | 0.47 (34) | |
| | EVI, LST _{scaled} | 0.50 (32) | | 0.45 (33) | |

[Title Page](#)
[Abstract](#)
[Introduction](#)
[Conclusions](#)
[References](#)
[Tables](#)
[Figures](#)

[Back](#)
[Close](#)
[Full Screen / Esc](#)
[Printer-friendly Version](#)
[Interactive Discussion](#)


Annual ET retrieved solely from satellites' Vis for the EM

D. Helman et al.

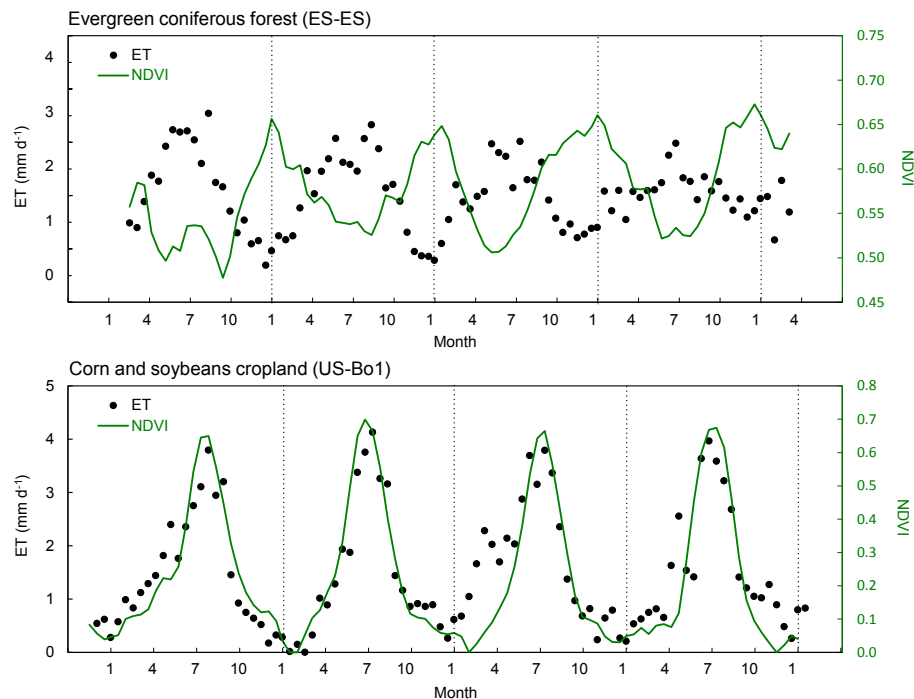


Figure 1. Sixteen-day averages of ET and 16 day MODIS-derived NDVI at two vegetation systems: PA, i.e. comprising perennial and annual vegetation (evergreen coniferous forest), and AN, i.e. annual vegetation alone (corn and soybean cropland). Note: NDVI in cropland site is the growing season NDVI, i.e. the minimum NDVI from each season was subtracted from the time series.

Title Page

Abstract

Introduction

Conclusions

References

Tables

Figures



Back

Close

Full Screen / Esc

Printer-friendly Version

Interactive Discussion



Annual ET retrieved solely from satellites' VIs for the EM

D. Helman et al.

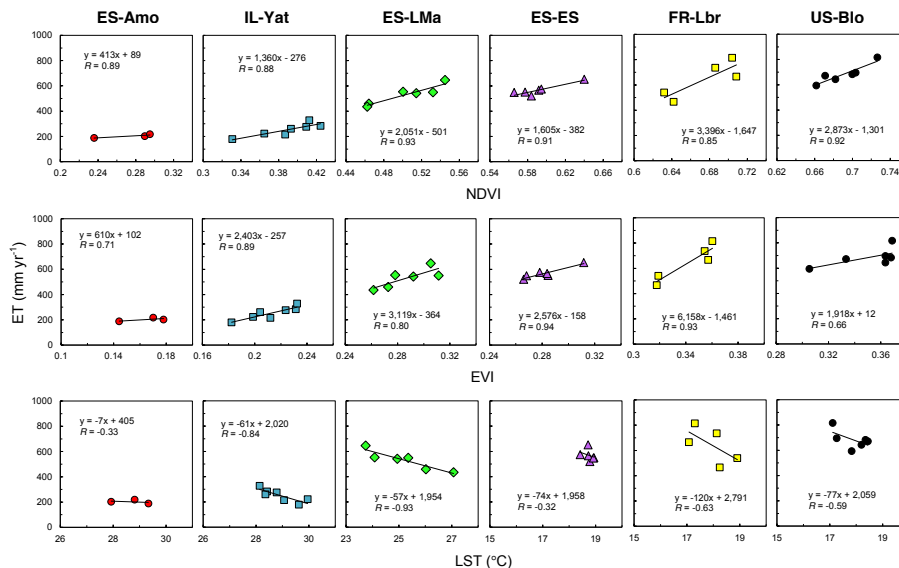


Figure 2. Relationships between total annual ET (mm yr⁻¹) from eddy covariance towers and mean annual MODIS-derived NDVI, EVI and daytime LST (LST, °C) in PA sites (perennials and annuals vegetation systems, i.e. forests, woodlands, savannah and shrublands).

Title Page

Abstract

Introduction

Conclusions

References

Tables

Figures



Back

Close

Full Screen / Esc

Printer-friendly Version

Interactive Discussion



Annual ET retrieved solely from satellites' VIs for the EM

D. Helman et al.

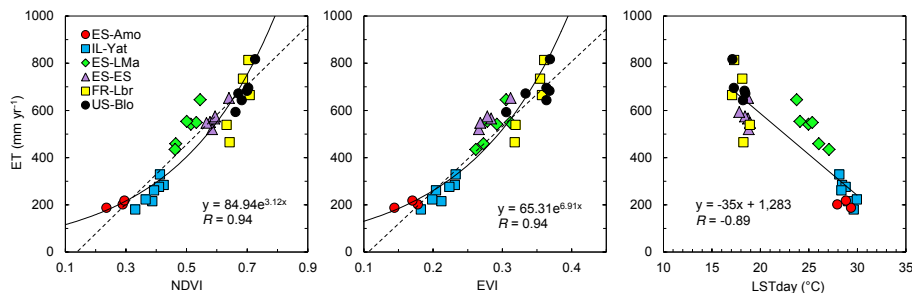


Figure 3. Same as Fig. 2 but for all PA sites together. The linear (dashed line) and exponential (solid line) functions are presented in ET–VIs with the R of the exponential function for ET–VIs.

Title Page

Abstract

Introduction

Conclusions

References

Tables

Figures



Back

Close

Full Screen / Esc

Printer-friendly Version

Interactive Discussion



Annual ET retrieved solely from satellites' Vis for the EM

D. Helman et al.

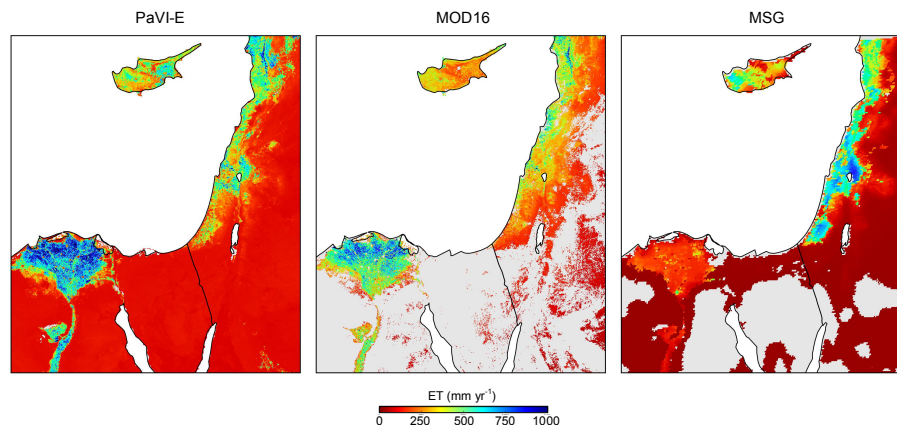


Figure 4. Maps of the total annual ET for the Eastern Mediterranean from PaVI-E, MODIS (MOD16) and MSG (LSA-SAF MSG ETa) for 2011. Grey colour indicates pixels with no data in MOD16 and MSG products.

[Title Page](#)[Abstract](#)[Introduction](#)[Conclusions](#)[References](#)[Tables](#)[Figures](#)[Back](#)[Close](#)[Full Screen / Esc](#)[Printer-friendly Version](#)[Interactive Discussion](#)

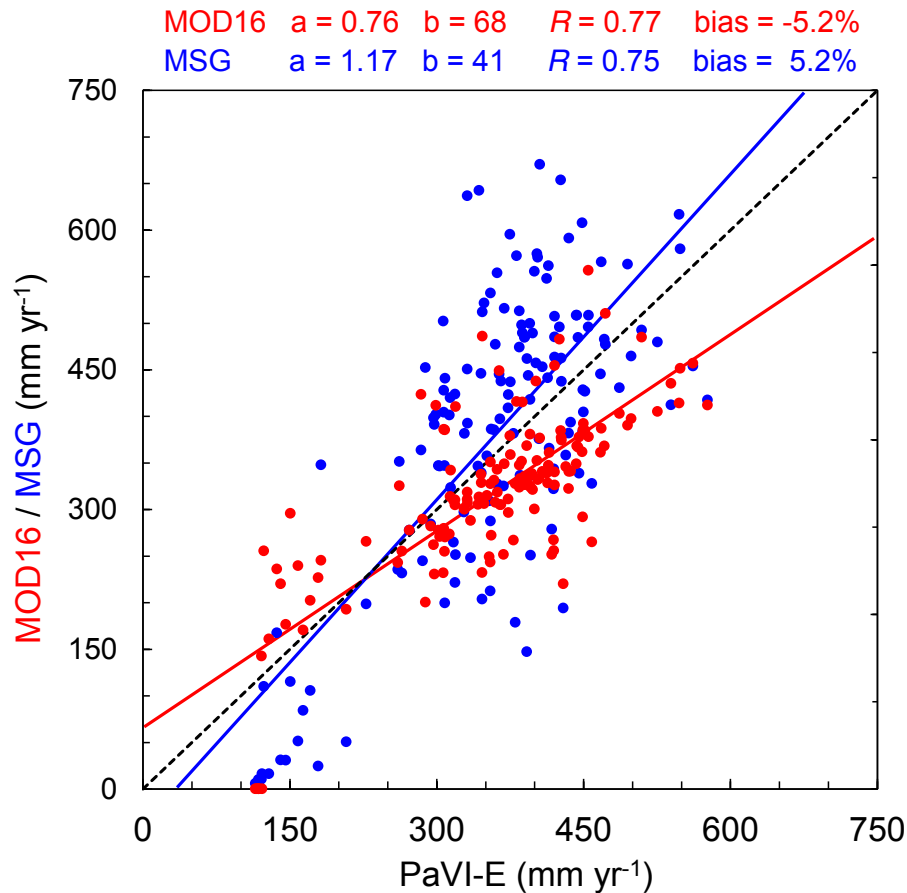


Figure 5. Total annual ET estimates at 148 Eastern Mediterranean basins (Fig. S1) from MODIS (MOD16) and MSG (LSA-SAF MSG ETa) vs. PaVI-E. Slope (a), intersection (b), Pearson's (R) and relative bias (bias/mean) are also presented. Dashed line indicates the 1 : 1 ratio.

Annual ET retrieved solely from satellites' Vis for the EM

D. Helman et al.

| | |
|--------------------------|--------------|
| Title Page | |
| Abstract | Introduction |
| Conclusions | References |
| Tables | Figures |
| ◀ | ▶ |
| ◀ | ▶ |
| Back | Close |
| Full Screen / Esc | |
| Printer-friendly Version | |
| Interactive Discussion | |



Annual ET retrieved solely from satellites' VIs for the EM

D. Helman et al.

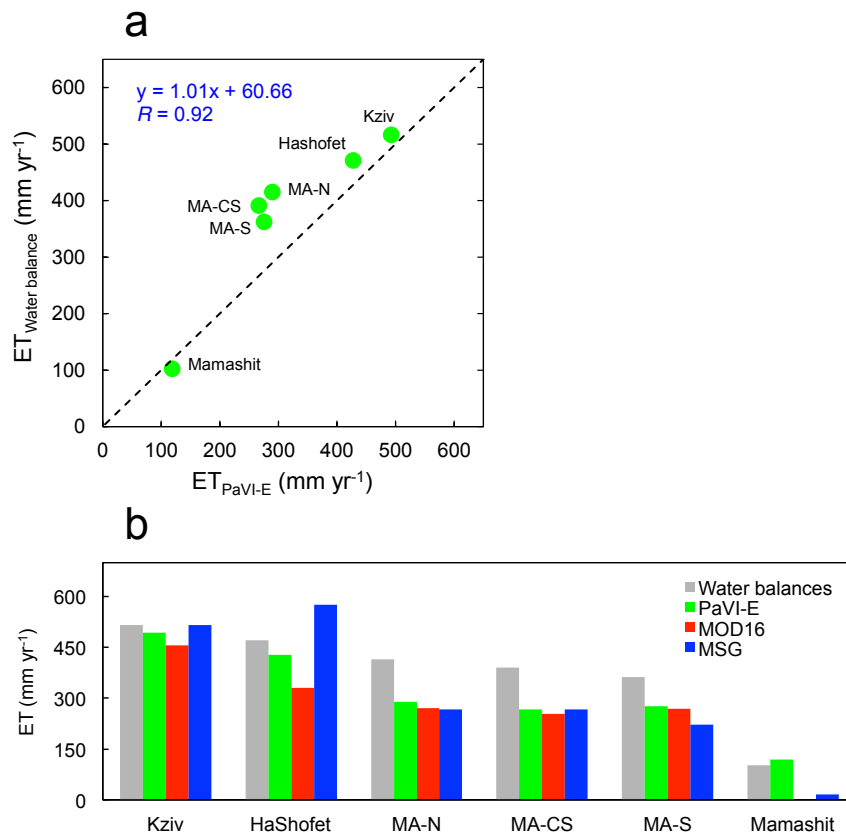


Figure 6. (a) Scatter plot of the mean total annual ET (2000–2013) retrieved from PaVI-E and calculated from water balances at six water catchments along the EM north–south rainfall gradient (Fig. S3). (b) Comparison between mean annual ET estimates from PaVI-E, MOD16, MSG and water balances in those six water catchments. MA-N, MA-CS and MA-S stand for north, centre-south, and south mountain aquifer, respectively.